Supplementary Information

High-performance and excellent thermal cycling stability of reversible protonic ceramic cells enabled by a promising Sr/Co-free $PrNi_{0.5}Fe_{0.5}O_{3-\delta}$ air electrode

Boseok Seong,[ab] Jiwon Yun,[ab] and Sihyuk Choi*[ab]

[a] Department of Mechanical Engineering, Kumoh National Institute of Technology, Gumi, Gyeongbuk, 39177, Republic of Korea

[b] Department of Aeronautics, Mechanical and Electronic Convergence Engineering, Kumoh National Institute of Technology, Gumi, Gyeongbuk, 39177, Republic of Korea

*E-mail: sh.choi@kumoh.ac.kr

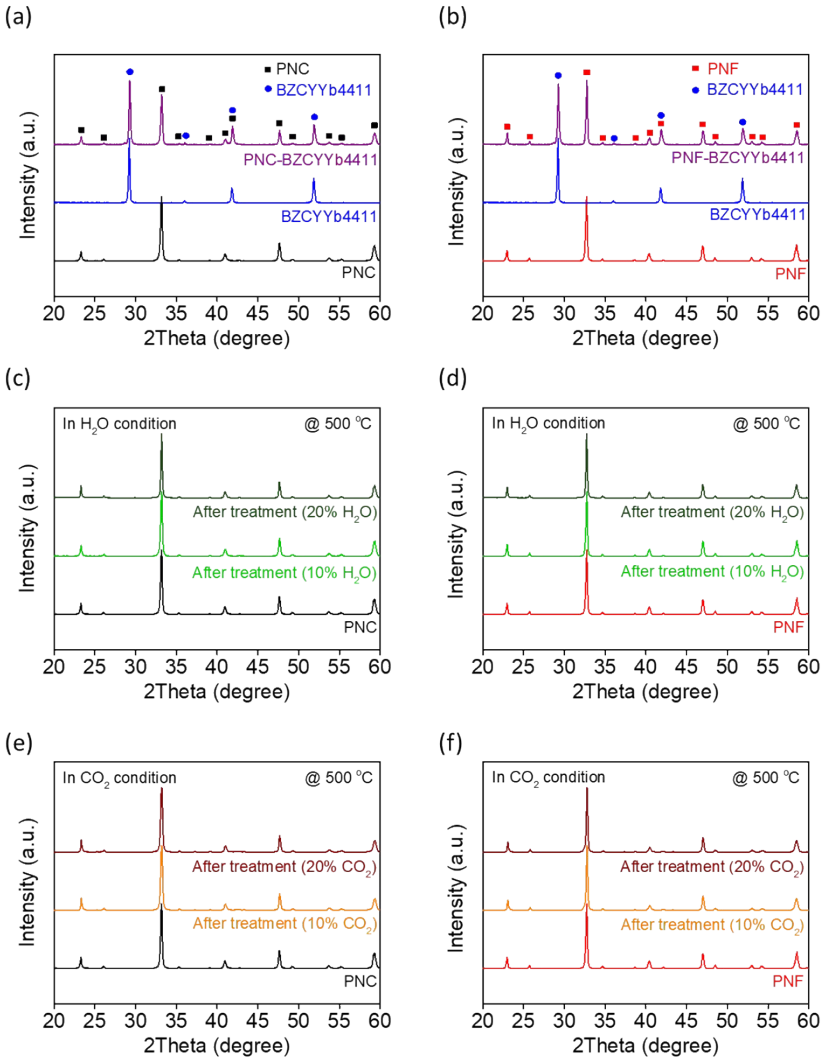

Fig. S1. Chemical compatibility between the (a) PNC and (b) PNF air electrode and BZCYYb4411 electrolyte after annealing at 950 °C for 4 h in air atmosphere. Post-treated the (c) PNC and (d) PNF air electrode after exposing to 10 and 20% H_2O. Post-treated the (e) PNC and (f) PNF air electrode after exposing to 10 and 20% CO_2 at 500 °C for 24 h.

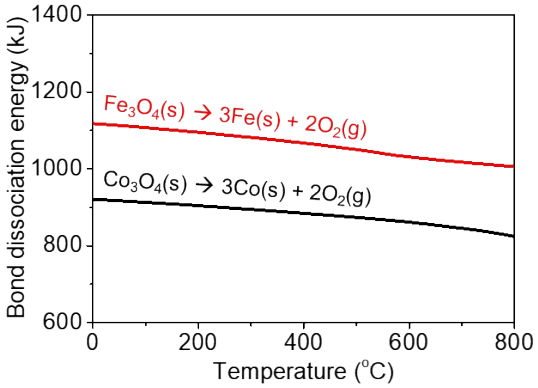

Fig. S2. Thermodynamic bond dissociation energy (BDE) calculations for Co-O and Fe-O bonds. Based on this definition, the BDEs of Co-O and Fe-O bonds in M_3O_4 (M = Co and Fe) structure were calculated as follows:

$$\Delta H_f\,(Bond\ dissociation\ energy) = \Delta H_f(Fe(s)) + \Delta H_f\big(O_2(g)\big) - \Delta H_f\big(Fe_3O_4(s)\big) \quad (1)$$

$$\Delta H_f\,(Bond\ dissociation\ energy) = \Delta H_f(Co(s)) + \Delta H_f\big(O_2(g)\big) - \Delta H_f\big(Co_3O_4(s)\big) \quad (2)$$

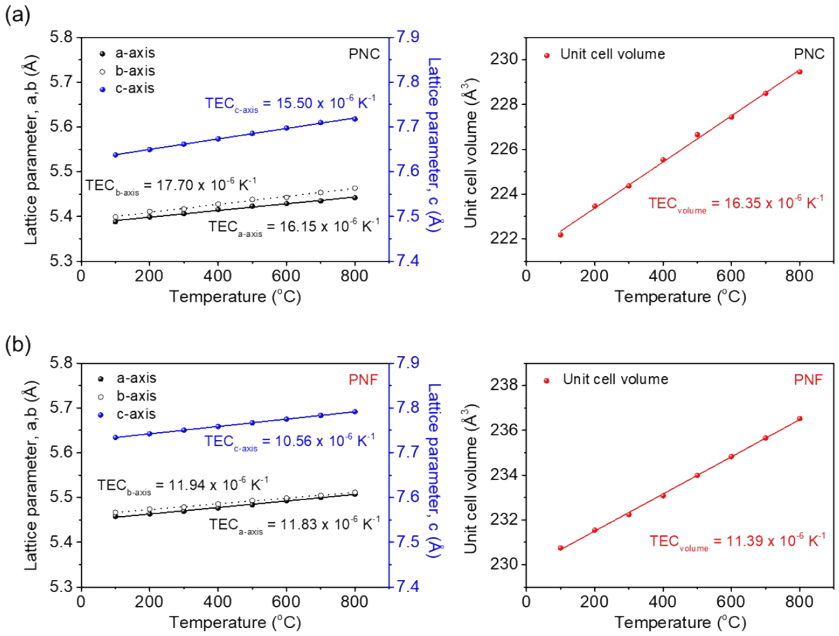

Fig. S3. (a) Lattice parameter changes and calculated TEC values of the PNC air electrode (b) Lattice parameter changes and calculated TEC values of the PNF air electrode at temperatures ranging from 100 to 800 °C.

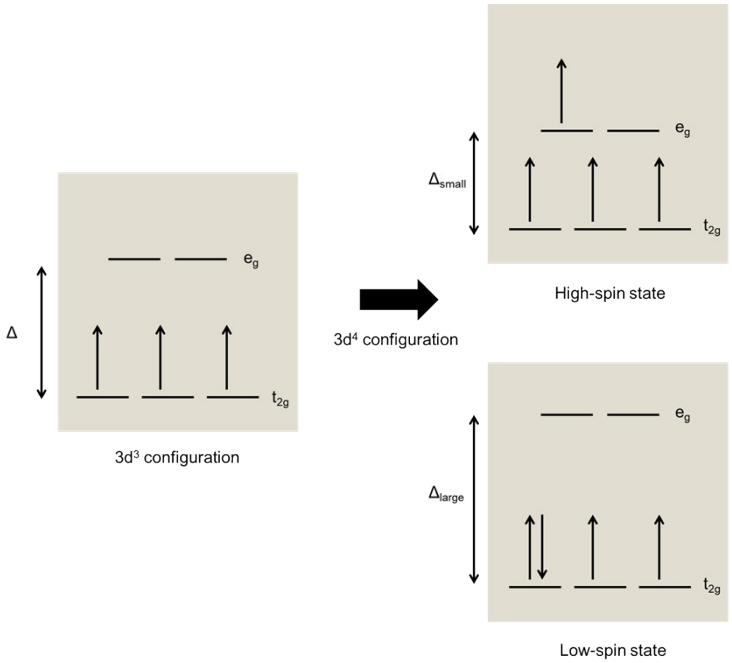

Fig. S4. Schematic electronic spin configurations for $3d^4$; high-spin state (Δ is small) and low-spin state (Δ is large).

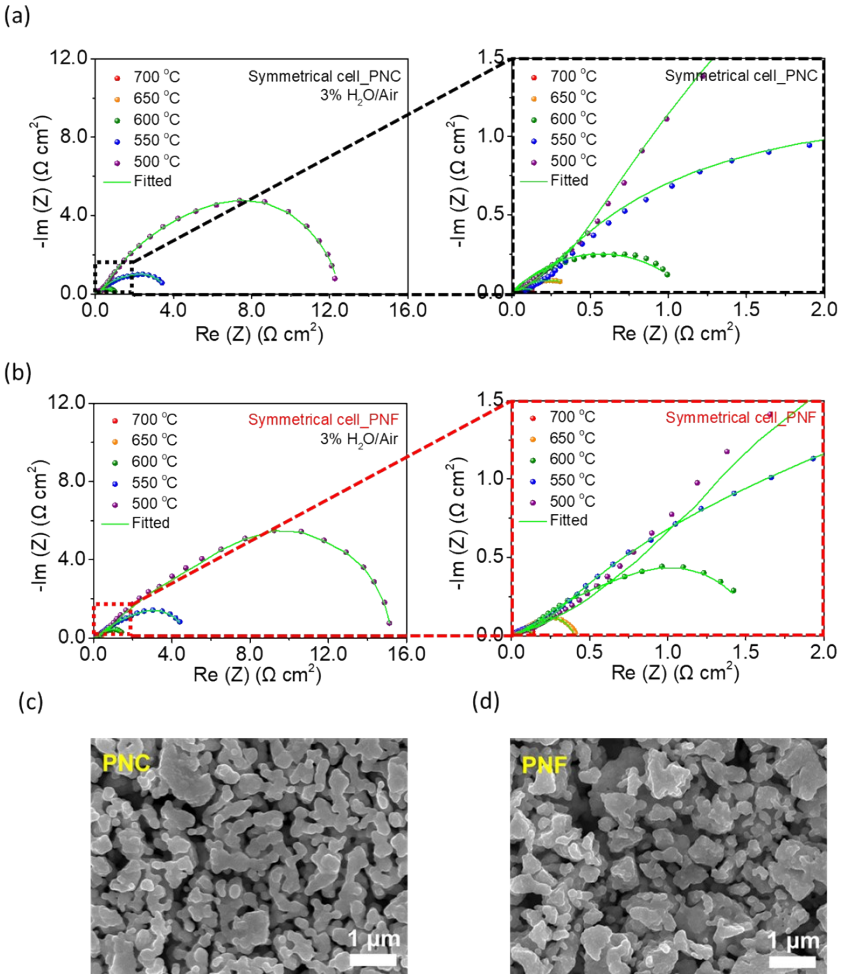

Fig. S5. EIS and fitted spectra of the BZCYYb4411-based symmetrical cells with the (a) PNC and (b) PNF air electrodes under open circuit voltage in temperature ranges of 500 to 700 °C in wet air (pH_2O=0.03 atm). Microstructures of the (c) PNC and (d) PNF air electrodes after sintering at 950 °C for 4 h in air atmosphere.

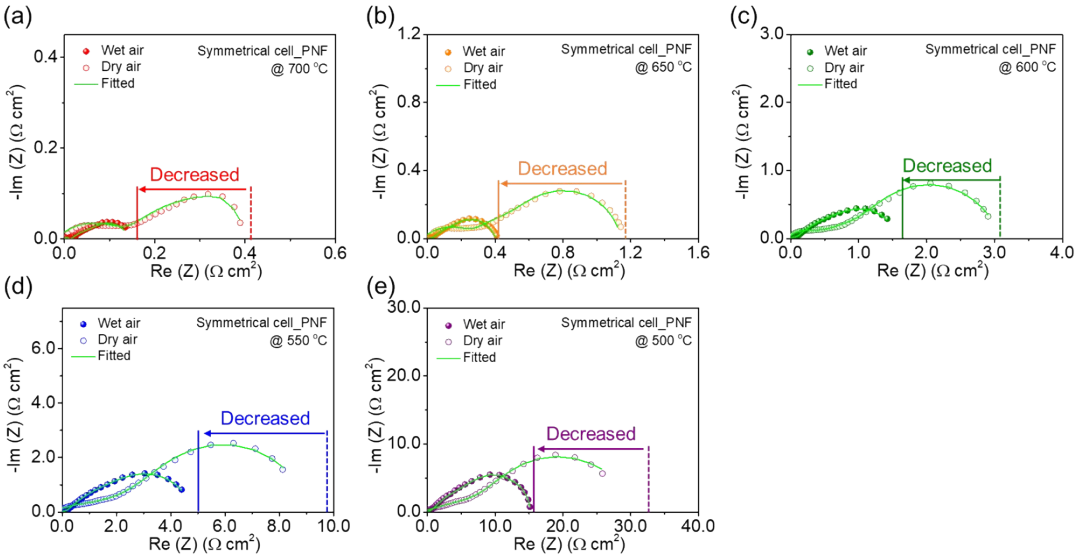

Fig. S6. EIS of the BZCYYb4411-based symmetrical cells with the PNF air electrode under open circuit voltage in temperature ranges of 500 to 700 °C in dry and wet air (pH$_2$O=0.03 atm).

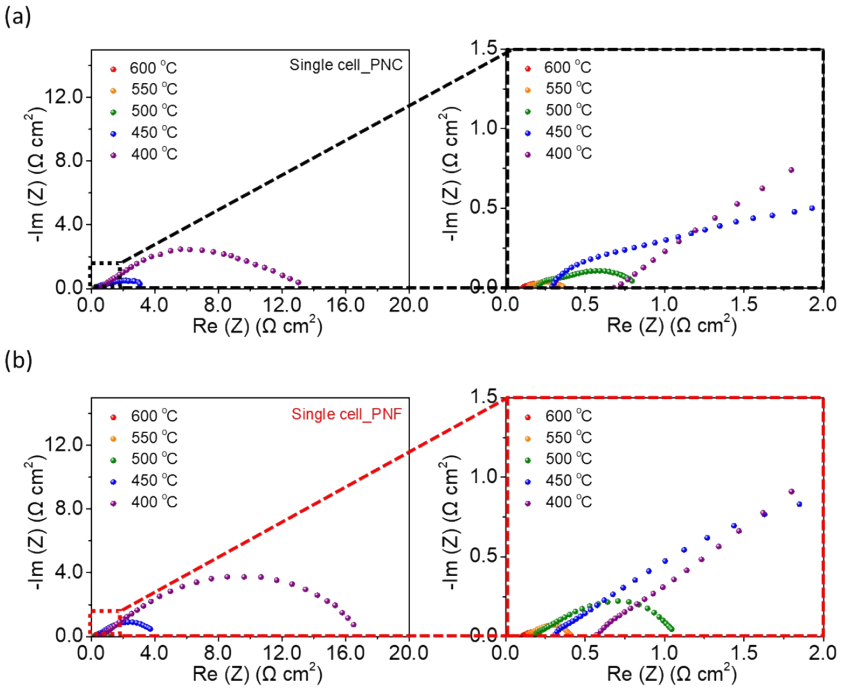

Fig. S7. EIS of the single cells with the (a) PNC and (b) PNF air electrodes under open circuit voltage in temperature ranges of 400 to 600 °C.

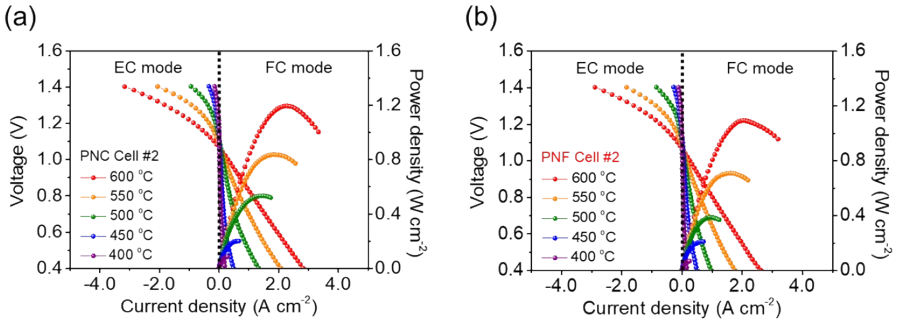

Fig. S8. *I–V* and *I–P* curves of the R-PCC single cells for #2 with (a) PNC and (b) PNF. Good reproducibility is obtained across the duplicate cells.

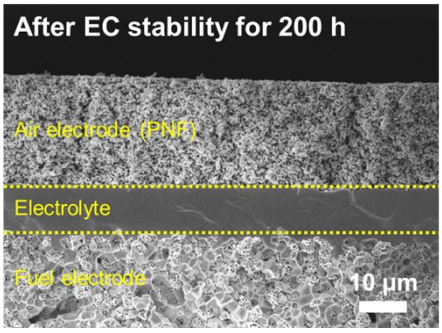

Fig. S9. Cross-sectional SEM images of PNF air electrode based R-PCC single cell following the EC stability for 200 h. No discernible microstructural changes were observed in R-PCC with the PNF air electrode before (**Fig. 5a**) and after EC stability measurement, particularly at the interfaces between the electrode and electrolyte.

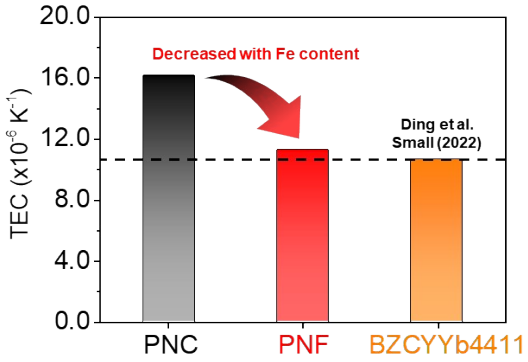

Fig. S10. Calculated TEC values of the PNC and PNF air electrodes from 200 to 900 °C and BZCYYb4411 electrolyte from 100 to 1000 °C.

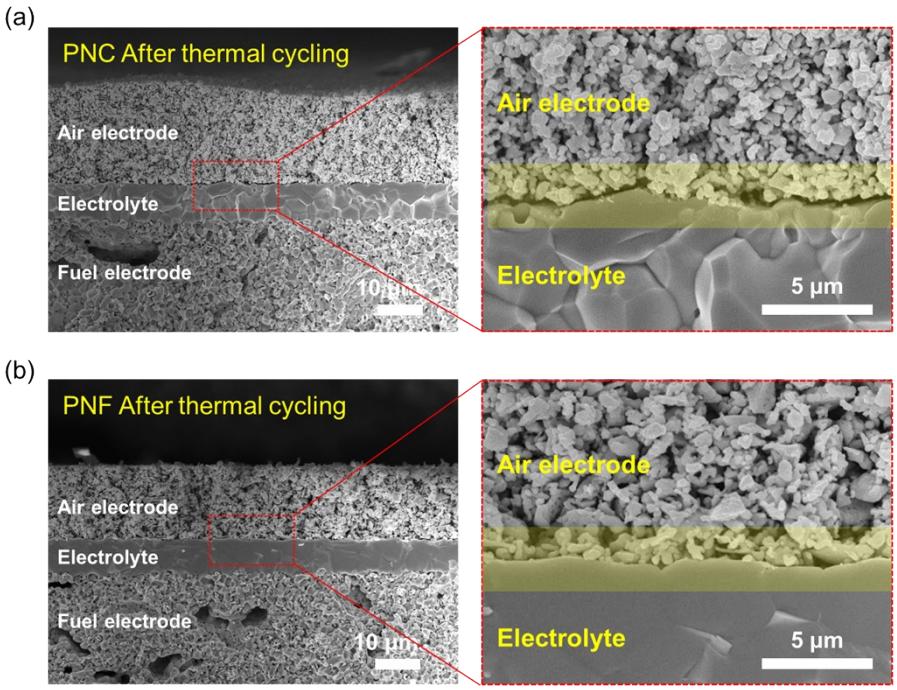

Fig. S11. After thermal cycling stability of single cells with the (a) PNC and (b) PNF air electrode.

Table S1. Binding energies of Pr 3d, Ni 2p, Co 2p, and Fe 2p.[1,2]

Element	Orbital	Binding energy (eV)
Pr	$3d_{5/2}$	931.8
	$3d_{3/2}$	952.2
Ni	$2p_{3/2}$	853.8
	$2p_{1/2}$	872.4
Co	$2p_{3/2}$	778.3
	$2p_{1/2}$	794.7
Fe	$2p_{3/2}$	709.7
	$2p_{1/2}$	723.1

Table S2. Valence distribution of the element of PNC and PNF air electrodes, derived from the XPS result.

Element	Oxidation state	Peak location (eV)	PNC		PNF	
			Fraction (%)	Average valence	Fraction (%)	Average valence
Pr	+3	927.1 932.3 947.1 953.0	92.7	+3.07	92.0	+3.08
	+4	928.5 949.1	7.3		8.0	
Ni	+2	853.9 866.8	67.8	+2.37	68.0	+2.36
	+3	856.0 870.5	27.6		27.7	
	+4	858.1	4.6		4.3	
Co	+2	778.2 792.8	13.4	+3.07	-	-
	+3	779.7 794.5	65.8		-	
	+4	781.7 796.2	20.8		-	
Fe	+2	707.4 720.8	-	-	8.6	+3.25
	+3	709.6 722.1	-		58.0	
	+4	712.2 724.3	-		33.4	

Table S3. O 1s XPS peak deconvolution results of PNC and PNF.

Air electrode	$O_O^\times$	$V_O^{\cdot\cdot}$	OH^-	H_2O	O_{ads}/O_{lat}
PNC	42.2%	10.1%	46.1%	1.6%	1.37
PNF	45.1%	6.7%	46.3%	1.9%	1.22

Table S4. Performance comparison of PNF air electrode with other reported Sr/Co-free air electrodes for PCFCs.

Air electrode	Electrolyte	Fuel electrode	Temp. (°C)	PPD (W cm^{-2})	Ref.
PNF ($PrNi_{0.5}Fe_{0.5}O_{3-\delta}$)	**BZCYYb4411 ($BaZr_{0.4}Ce_{0.4}Y_{0.1}Yb_{0.1}O_{3-\delta}$)**	**Ni-BZCYYb4411**	**600**	**1.17**	**This work (Cell #1)**
			550	**0.70**	
			500	**0.41**	
			450	**0.23**	
			400	**0.07**	
			600	**1.09**	**This work (Cell #2)**
			550	**0.71**	
			500	**0.39**	
			450	**0.21**	
			400	**0.07**	
$BFSBi_{0.3}$ ($BaFe_{0.5}Sn_{0.2}Bi_{0.3}O_{3-\delta}$)	BZCY ($BaZr_{0.1}Ce_{0.7}Y_{0.2}O_{3-\delta}$)	Ni-BZCY	600	0.84	[3]
			550	0.65	
			500	0.43	
			450	0.29	
			400	0.12	
BCYF2 ($BaCe_{0.16}Y_{0.04}Fe_{0.8}O_{3-\delta}$)	BZCYYb1711 ($BaZr_{0.1}Ce_{0.7}Y_{0.1}Yb_{0.1}O_{3-\delta}$)	Ni-BZCYYb1711	600	0.66	[4]
			550	0.49	
			500	0.30	
			450	0.15	
PBCF ($PrBa_{0.8}Ca_{0.2}Fe_2O_{6-\delta}$)	BZCYYb1711	Ni-BZCYYb1711	600	0.44	[5]
PBCFC ($PrBa_{0.8}Ca_{0.2}Fe_{1.8}Ce_{0.2}O_{6-\delta}$)	BZCYYb1711	Ni-BZCYYb1711	600	0.87	
PNC ($Pr_2Ni_{0.8}Cu_{0.2}O_{4+\delta}$)	BZCYYb1711	Ni-BZCYYb1711	600	0.24	[6]
			550	0.16	
BLFZ-BZCYYb1711	BZCYYb1711	Ni-BZCYYb1711	600	0.09	[7]

($Ba_{0.95}La_{0.05}Fe_{0.8}Zn_{0.2}O_{3-\delta}$ -BZCYYb1711)					
BFSBi ($BaFe_{0.5}Sn_{0.2}Bi_{0.3}O_{3-\delta}$)	BZCYYbF ($BaZr_{0.3}Ce_{0.48}Fe_{0.02}Y_{0.1}Yb_{0.1}O_{3-\delta}$)	Ni- BZCYYbF	600	0.28	[8]
BFSBi95 ($Ba_{0.95}Fe_{0.5}Sn_{0.2}Bi_{0.3}O_{3-\delta}$)	BZCYYbF	Ni- BZCYYbF	600	0.36	
PBNZ1 ($Pr_{1.8}Ba_{0.2}Ni_{0.9}Zn_{0.1}O_{4+\delta}$)	BZCY	Ni-BZCY	600 550	0.44 0.23	[9]
$(PL)_{1.9}$NCMn nanofiber ($((Pr_{0.9}La_{0.1})_{1.9}(Ni_{0.7}Cu_{0.3})_{0.9}Mn_{0.1}O_{4+\delta}$)	BZCY	Ni-BZCY	600 550	0.53 0.38	[10]
BCF82 ($Ba_{0.8}Ca_{0.2}FeO_{3-\delta}$)	BZCYYb1711	Ni-BZCYYb1711	600	0.73	[11]

Table S5. Performance comparison of PNF air electrode with other reported Sr/Co-free air electrodes for PCECs.

Air electrode	Electrolyte	Fuel electrode	Temp. (°C)	Current density at 1.3 V (A cm^{-2})	Ref.
PNF	**BZCYYb4411**	**Ni-BZCYYb4411**	**600**	**-1.78**	**This work (Cell #1)**
			550	**-0.95**	
			500	**-0.35**	
			450	**-0.15**	
			400	**-0.06**	
			600	**-1.61**	**This work (Cell #2)**
			550	**-0.88**	
			500	**-0.35**	
			450	**-0.12**	
			400	**-0.04**	
PBCF	BZCYYb1711	Ni-BZCYYb1711	600	-0.94	[5]
PBCFC	BZCYYb1711	Ni-BZCYYb1711	600	-1.73	
PNC	BZCYYb1711	Ni-BZCYYb1711	600	-0.32	[6]
			550	-0.22	
BLFZ-BZCYYb1711	BZCYYb1711	Ni-BZCYYb1711	600	-0.26	[7]
BFSBi	BZCYYbF	Ni-BZCYYbF	600	-0.40	[8]
BFSBi95	BZCYYbF	Ni-BZCYYbF	600	-0.51	
PBNZ1	BZCY	Ni-BZCY	600	-0.83	[9]
			550	-0.34	
$(PL)_{1.9}$NCMn nanofiber	BZCY	Ni-BZCY	600	-0.70	[10]
			550	-0.47	
BCF82	BZCYYb1711	Ni-BZCYYb1711	600	-1.21	[11]
PNO-BZCY262 ($Pr_2NiO_{4+\delta}$-$BaZr_{0.2}Ce_{0.6}Y_{0.2}O_{3-\delta}$)	BZCY262	Ni-BZCY262	600	-0.35	[12]
			550	-0.23	
PLNCu-BZCY ($(Pr_{0.9}La_{0.1})_2(Ni_{0.8}Cu_{0.2})O_{4+\delta}$-BZCY)	BZCY	Ni-BZCY	600	-0.28	[13]

References

1. B. V. Crist, *J. Electron Spectros. Relat. Phenomena*, 2019, **231**, 75–87.
2. G. Greczynski and L. Hultman, *Prog. Mater. Sci.*, 2020, **107**, 100591.
3. Y. Xia, Z. Jin, H. Wang, Z. Gong, H. Lv, R. Peng, W. Liu and L. Bi, *J. Mater. Chem. A*, 2019, **7**, 16136–16148.
4. D. Zou, Y. Yi, Y. Song, D. Guan, M. Xu, R. Ran, W. Wang, W. Zhou and Z. Shao, *J. Mater. Chem. A*, 2022, **10**, 5381–5390.
5. T. Hu, F. Zhu, J. Xia, F. He, Z. Du, Y. Zhou, Y. Liu, H. Wang and Y. Chen, *Adv. Funct. Mater.*, 2023, **33**, 2305567.
6. A. P. Tarutin, Y. G. Lyagaeva, A. I. Vylkov, M. Y. Gorshkov, G. K. Vdovin and D. A. Medvedev, *J. Mater. Sci. Technol*., 2021, **93**, 157–168.
7. J. Jing, Z. Lei, Z. Zheng, H. Wang, P. Zhang, Z. Wang, H. Xu and Z. Yang, *Int. J. Hydrogen Energy*, 2023, **48**, 9037–9045.
8. Z. Zhu, M. Zhou, Z. Fan, Q. Wu, K. Tan, Y. Liu, Y. Chen and J. Liu, *ACS Appl. Energy Mater.*, 2023, **6**, 5155–5166.
9. L. Yang, X. Ren, W. Peng, A. Wang, D. Yan, J. Li and L. Jia, *J. Power Sources*, 2023, **586**, 233652.
10. G. Xue, J. Li, H. Wang, H. Sun, X. Guo and Q. Hu, *J. Power Sources*, 2022, **552**, 232220.
11. G. Zhang, T. Chen, Y. Yao, C. Wang, X. Bao, G. Zheng, Z. Huang, X. Zhang, K. Liu, L. Xu, Y. Zhou and S. Wang, *Appl. Catal. B: Environ.*, 2024, **355**, 124176.
12. W. Li, B. Guan, L. Ma, S. Hu, N. Zhang and X. Liu, *J. Mater. Chem. A*, 2018, **6**, 18057–18066.
13. W. Wang, Y. Li, Y. Liu, Y. Tian, B. Ma, J. Li, J. Pu and B. Chi, *ACS Sustainable Chem. Eng.*, 2021, **9**, 10913–10919.